MODELING OF PULVERIZED COAL AND BIOMASS CO-FIRING IN A 150 KW SWIRLING-STABILIZED BURNER AND EXPERIMENTAL VALIDATION

Chungen YIN*, **Søren Knudsen KÆR***, **Lasse ROSENDAHL*** and **Søren Lovmand HVID****

*Dept. of Energy Technology, Aalborg University, Pontoppidanstraede 101, 9220 Aalborg East, Denmark
**DONG Energy, Kraftværksvej 53, 7000 Fredericia, Denmark

ABSTRACT   A comprehensive CFD modeling study has been undertaken to investigate the co-firing of pulverized coal and biomass in a 150 kW_{Fuel} swirl-stabilized burner, which is similar in flow pattern to a typical low-NO_x burner. The objective of the present study is to derive a reliable modeling methodology for design and optimization of low NO_x burners co-firing pulverized coal and biomass. For this purpose, the effects of meshes, global reaction mechanisms for homogeneous combustion, turbulence models, turbulence-chemistry interactions, properties of the solid fuels, and solid-fuel particle conversion models are finely examined. The modeling results are compared with detailed mapping of molar fractions of main species, obtained from FT-IR and a Horiba gas analyzer. This paper presents mainly the comparison of different global homogenous combustion mechanisms and different solid-fuel particle conversion models, in modeling of pulverized coal and biomass co-combustion.

Keywords: Biomass, Coal, Co-combustion, CFD, Swirl burner, Global reaction mechanism, Particle conversion

1. INTRODUCTION

Biomass fuels are one of the most important energy resources and are also considered environmentally friendly and renewable, which has greatly spurred interest in using biomass for heat and power production in order to mitigate the problems of global warming and the limited availability of fossil fuels. Co-firing biomass in existing pulverized coal-fired power plants is one of the main options currently used in biomass combustion for energy production. Most pulverized-coal boilers use low-NO_x burners, which are optimized to reduce NO emission while maintaining complete coal-burnout. Replacing a fuel or even changing a small portion of the fuel may upset this optimization [1].

This paper presents a comprehensive CFD modeling study of co-firing pulverized coal and biomass in a 150 kW_{Fuel} swirl-stabilized burner, which is similar in flow pattern to a typical low NO_x burner. The modeling results are compared with the experimental data, measured by FT-IR and a Horiba gas analyzer. Due to editorial limits, this paper highlights mainly the effects of different global reaction mechanisms for the volatiles of the solid fuels, and different models for the solid-fuel particle conversion.

2. EXPERIMENTAL WORKS

Under the framework of the same project, all the experimental works were done in a burner flow reactor, located in Brigham Young University. A scaled cross-section view of the inner chamber of the reactor indicating locations of the burner quarl and access windows is shown in Fig. 1. The reactor has a vertical height of 240 cm, and an inner diameter of 75 cm. The dual-feed swirl burner (not shown in Fig. 1) fires the fuels downward (down-fired) from the top of the reactor, with a self-sustaining flame. The combustion products pass through an ash separator and scrubber before being vented into the air. The main measuring effort was to produce high quality, quantitative

maps of gas species (CO_2, CO, H_2O, O_2; CH_4, C_2H_2, C_2H_4, C_6H_6; NO, NH_3, HCN) in the flame. The coordinate system (z, r) in Fig. 1 shows the measuring grid. All the details, including the burner and reactor, firing conditions and measured species maps, can be found in [2].
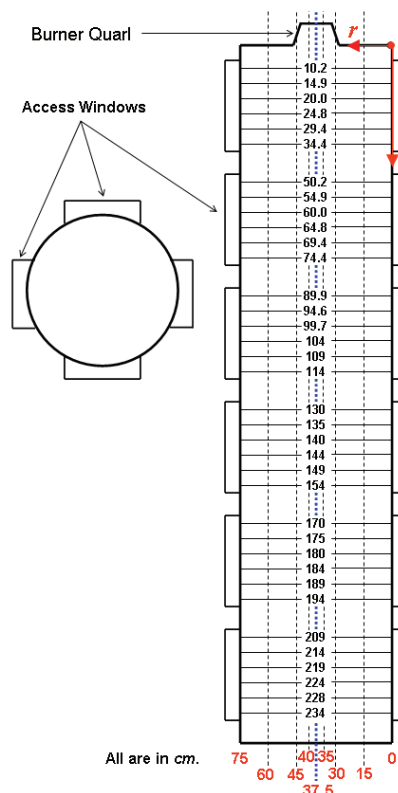

Fig. 1 A scaled view of the reactor interior.

The fuels and the operational conditions of co-firing pulverized coal and biomass are given in Table 1.
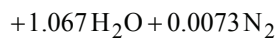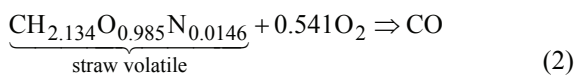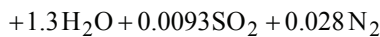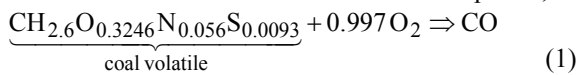
Table 1 Fuels and operational conditions

	Coal	Straw
Proximate analysis		
Moisture [wt%, as received]	2.1	7.7
Fixed carbon [wt%, dry]	51.5	15.6
Volatiles [wt%, dry]	40.6	79.5
Ash [wt%, dry]	7.89	4.91
HHV [kJ/kg, dry]	30731	18493
Ultimate analysis		
C [wt%, dry]	74.8	47.3
H [wt%, dry]	5.08	5.68
N [wt%, dry]	1.53	0.54
O [wt%, dry]	10.1	41.6
S [wt%, dry]	0.58	<0.01
Particle Rosin-Rammler parameters		
Min. diameter [μm]	25	50
Max. diameter [μm]	200	1000
Mean diameter [μm]	110.4	451.0
Spread parameter [-]	4.40	2.31

Operational parameters					
Center fuel [kg/s]	Annular fuel [kg/s]	Center air [kg/s]	Annular air [kg/s]	Secondary air [kg/s]	Swirling number
0.004194 (straw)	0.002083 (coal)	0.0025	0.003333	0.044444	1

3. CFD MODELING

Compared with pulverized coal particles, straw particles are relatively big in size, light in density, and non-spherical in shape, which greatly affect the motion and conversion of fuel particles in combustors [3]. In this work, the effect of non-sphericity of the fuel particles on their motion and conversion has not been accounted for. Both the coal and straw particles are assumed to be spherical. When the fuel particles travel through gas and interact with gas in the reactor, they heat up, devolatilize and undergo char combustion, creating sources for reaction in gas phase. Two different ways are used for the gas phase combustion of the fuel-volatiles. Two different methods are also employed for the conversion of the relatively big straw particles. All the CFD simulations (62600 cells, steady, axisymmetric swirl) are done using FLUENT v.6.3.26 [4]. The user-defined sub-models are implemented into the code via UDFs.
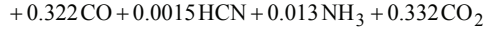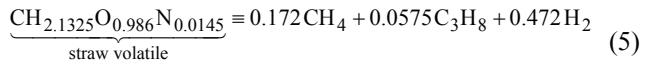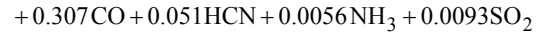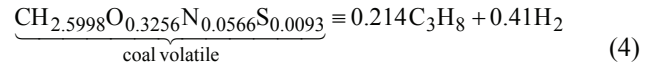
3.1 Global reaction mechanisms for volatile combustion

Mechanism-1 (the simplified 2-step global reaction mechanism). Two "artificial" species are used to represent the coal-volatile and straw-volatile, respectively. The combustion of the two volatiles is modeled using Finite Rate / Eddy Dissipation Model (EDM) and a two-step reaction mechanism with CO as the intermediate species,
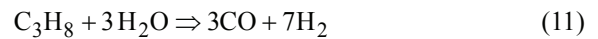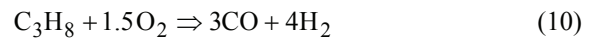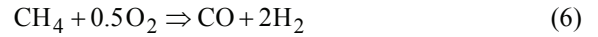
$$\underbrace{CH_{2.6}O_{0.3246}N_{0.056}S_{0.0093}}_{coal\ volatile} + 0.997\,O_2 \Rightarrow CO$$
$$+ 1.3\,H_2O + 0.0093\,SO_2 + 0.028\,N_2 \quad (1)$$

$$\underbrace{CH_{2.134}O_{0.985}N_{0.0146}}_{straw\ volatile} + 0.541\,O_2 \Rightarrow CO$$
$$+ 1.067\,H_2O + 0.0073\,N_2 \quad (2)$$

$$CO + 0.5\,O_2 \Rightarrow CO_2 \quad (3)$$

The compositions and formation enthalpies of the two "volatiles" are determined from the proximate and ultimate analysis data of coal and straw, respectively. There are 8 species and 3 reactions, Eq.(1)~(3), in this mechanism.

Mechanism-2 (the global mechanism of Jones and Lindstedt). The two volatiles are considered as a mixture of real species, as shown in Eq. (4) and (5), respectively.

$$\underbrace{CH_{2.5998}O_{0.3256}N_{0.0566}S_{0.0093}}_{coal\ volatile} \equiv 0.214\,C_3H_8 + 0.41\,H_2$$
$$+ 0.307\,CO + 0.051\,HCN + 0.0056\,NH_3 + 0.0093\,SO_2 \quad (4)$$

$$\underbrace{CH_{2.1325}O_{0.986}N_{0.0145}}_{straw\ volatile} \equiv 0.172\,CH_4 + 0.0575\,C_3H_8 + 0.472\,H_2$$
$$+ 0.322\,CO + 0.0015\,HCN + 0.013\,NH_3 + 0.332\,CO_2 \quad (5)$$

Then the global reaction mechanisms, proposed by Jones and Lindstedt (1988) for hydrocarbon combustion [5], are used for combustion of the hydrocarbons (i.e., CH_4 and C_3H_8) in the mixture. The turbulence-chemistry interaction is modeled by Eddy-Dissipation Concept (EDC).

$$CH_4 + 0.5\,O_2 \Rightarrow CO + 2\,H_2 \quad (6)$$
$$CH_4 + H_2O \Rightarrow CO + 3\,H_2 \quad (7)$$
$$H_2 + 0.5\,O_2 \Leftrightarrow H_2O \quad (8)$$
$$CO + H_2O \Leftrightarrow CO_2 + H_2 \quad (9)$$
$$C_3H_8 + 1.5\,O_2 \Rightarrow 3\,CO + 4\,H_2 \quad (10)$$
$$C_3H_8 + 3\,H_2O \Rightarrow 3\,CO + 7\,H_2 \quad (11)$$

In this mechanism, there are 12 species in total (H_2, H_2O, O_2, NO, HCN, NH_3, CH_4, C_3H_8, CO, CO_2, SO_2, N_2) and 6 gas-phase reactions, Eq.(6) – Eq.(11).

In the above two different mechanisms, the global rate expressions for the 9 involved reactions are given as,

$$r_1^f = k_1^f(T) \cdot [vol\_coal]^{0.2} \cdot [O_2]^{1.3} \quad (12)$$
$$r_2^f = k_2^f(T) \cdot [vol\_straw]^{0.2} \cdot [O_2]^{1.3} \quad (13)$$
$$r_3^f = k_3^f(T) \cdot [CO] \cdot [O_2]^{0.25} \quad (14)$$
$$r_6^f = k_6^f(T) \cdot [CH_4]^{0.5} \cdot [O_2]^{1.25} \quad (15)$$
$$r_7^f = k_7^f(T) \cdot [CH_4] \cdot [H_2O] \quad (16)$$
$$r_8^f = k_8^f(T) \cdot [H_2]^{0.25} \cdot [O_2]^{1.5} \quad (17)$$
$$r_9^f = k_9^f(T) \cdot [CO] \cdot [H_2O] \quad (18)$$
$$r_{10}^f = k_{10}^f(T) \cdot [C_3H_8]^{0.5} \cdot [O_2]^{1.25} \quad (19)$$
$$r_{11}^f = k_{11}^f(T) \cdot [C_3H_8] \cdot [H_2O] \quad (20)$$

in which the reaction rate coefficients can be expressed as

$$k_i^f(T) \equiv A \cdot T^b \cdot \exp(-E/(R_u T)), \quad (21)$$

with the kinetic parameters given in Table 2.

Table 2 Kinetic parameters for the gas-phase reactions

Reaction	Rate coefficient	A	b	E [J/kmol]
1	$k_1^f(T)$	2.119×10^{11}	0	2.027×10^8
2	$k_2^f(T)$	2.119×10^{11}	0	2.027×10^8
3	$k_3^f(T)$	2.239×10^{12}	0	1.7×10^8
6	$k_6^f(T)$	4.4×10^{11}	0	1.26×10^8
7	$k_7^f(T)$	3×10^8	0	1.26×10^8
8	$k_8^f(T)$	6.8×10^{15}	-1	1.67×10^8
9	$k_9^f(T)$	2.75×10^9	0	8.4×10^7
10	$k_{10}^f(T)$	4×10^{11}	0	1.26×10^8
11	$k_{11}^f(T)$	3×10^8	0	1.26×10^8

3.2 Conversion of big straw particles

Conversion of solid fuel particles is modeled by DPM (Discrete Phase Model) laws. Under the traditional conditions in a pulverized coal/biomass co-fired combustor, the Biot number of pulverized coal particles is well below 0.1, and coal particles are under isothermal conditions. However, for big biomass particles, the Biot number is above 0.1, indicating that isothermal conditions may not hold any more [6]. For comparison, two different ways are used for the conversion of big straw particles in the reactor.

Default DPM laws. The particle is treated as a lumped system: different conversion processes (e.g., drying, devolatilization, char oxidation) occur in series. For example, volatile release begins only after all the moisture is driven off and the temperature of the particle reaches the vaporization temperature. This is the default way used in FLUENT to update the mass, temperature, size and density of a combusting particle when it travels in a combustor [4].

Custom DPM laws. The big straw particles are discretized into a number of shells. For each of the shells, temperature, conversion rates and compositions will be updated. By using the custom DPM laws, the different conversion processes occur in parallel, with the conversion fronts moving from the surface to the center of the particle. Basically, the custom DPM laws are similar in mechanism with intra-particle heat, momentum and mass transport modeling, e.g., in [7]. Here only a conceptual comparison between the default and the custom DPM laws is sketched in Fig. 2.
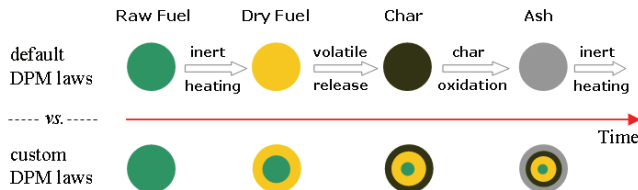

Fig. 2 Conceptual comparison of different DPM laws.

3.3 Summary of five different cases

Table 3 briefly summarizes the five different cases, whose results are presented in this paper.

Table 3 Main mechanisms/models used in the five cases.

Case label	Volatile combustion	Straw particle conversion	Other models
traditional	Mechanism-1	default DPM law	RKE (Realizable k-ε) for turbulence; DO for radiation
SKE-default	Mechanism-2	default DPM law	SKE (Standard k- ε); DO for radiation
SKE-custom	Mechanism-2	custom DPM law	SKE for turbulence; DO for radiation
RKE-default	Mechanism-2	default DPM law	SKE for turbulence; DO for radiation
RKE-custom	Mechanism-2	custom DPM law	RKE for turbulence; DO for radiation

4. CALIBRATION OF UDFS AND CFD MODELING

Before being compared with the experimental data, the UDFs (e.g., the UDF for gas species sources from particles which is used for global reaction mechanism-2; the UDF for the custom DPM laws) and the CFD modeling have been calibrated, against the expectation or in terms of overall heat/mass/element balance. As a demonstration, Table 4 lists part of the calibration results for 2 of the cases. One may conclude from Table 4 that the UDFs work properly in terms of species sources and both the cases are well converged. For the case "RKE-default", in which the default DPM laws are used for both coal and straw particles, the error with the H_2O source is relatively big (about -2.5%), which was proven to have nothing to do with the species source UDF and is likely an inherent problem with wet combustion of fuel particles. The comparison also shows the custom laws produce a higher DPM enthalpy source than the default laws. This difference is greater than what one could expect from the difference in the char conversion rates, hinting that the custom DPM laws may need to be locally refined for the heat generation and transfer.

Table 4 Part of the calibration results.

(1) Calibration of the DPM source UDF					
DPM source	Expected value [kg/s]	RKE-default		RKE-custom	
		FLUENT report, kg/s	Relative Error, %	FLUENT report, kg/s	Relative Error,%
H_2 source	1.2986e-4	1.3011e-4	0.187	1.2986e-4	-0.001
HCN source	5.8209e-5	5.8217e-5	0.014	5.8207e-5	-0.003
NH_3 source	2.6759e-5	2.6816e-5	0.215	2.6759e-5	-0.001
CH_4 source	2.8260e-4	2.8331e-4	0.251	2.8260e-4	0.000
C_3H_8 source	6.3252e-4	6.3316e-4	0.101	6.3251e-4	-0.002
CO source	1.2616e-3	1.2639e-3	0.182	1.2616e-3	-0.001
SO_2 source	2.3653e-5	2.3652e-5	-0.004	2.3652e-5	-0.004
H_2O source	3.6672e-4	3.5747e-4	-2.523	3.6710e-4	0.102
CO_2 source	7.5526e-3*	6.5107e-3		6.3746e-3	
(2) Calibration of the overall mass balance					
DPM mass source [kg/s]		0.0056399		0.0056056	
Net mass flux over all the boundaries [kg/s]		-0.0056429		-0.0056056	
Relative error [%]		-0.0539		0.0000	
(3) Calibration of the overall heat balance					
DPM enthalpy source[W]		-30821		-42841	
Net total heat flux over all the boundaries [W]		30780		42947	
Relative error [%]		0.1348		-0.2460	

* it's the maximum value corresponding to 100% char conversion; O_2 source and others are not given here.

5. CFD VALIDATION WITH EXPERIMENTAL DATA

The detailed gas species were measured at the grid points (6×6=36 along the axis direction; 9 along the radial direction, as shown in Fig. 1). Figure 3 and Figure 4 show the comparison between the measured main species and the CFD predicted values on two representative measuring lines, *y=0.075m* and *y=0.225m*, respectively.

- The CFD results show a generally acceptable agreement with the measured data, except for CO mole fraction, in particular on the line *y=0.225m* where CO concentration is too low to be measured accurately.

- RKE makes a much bigger difference with SKE in the core region than in the near-wall region (i.e., Fig. 3 *vs.* Fig. 4), just as expected. For combusting swirling flows, the fidelity of CFD modeling is mainly determined by the accuracy of the turbulence model in the core region, rather than in the near-wall zone.

- The custom DPM laws make quite significant difference with the default DPM laws in the predicted gas species, especially in the core zone, which is out of expectation.
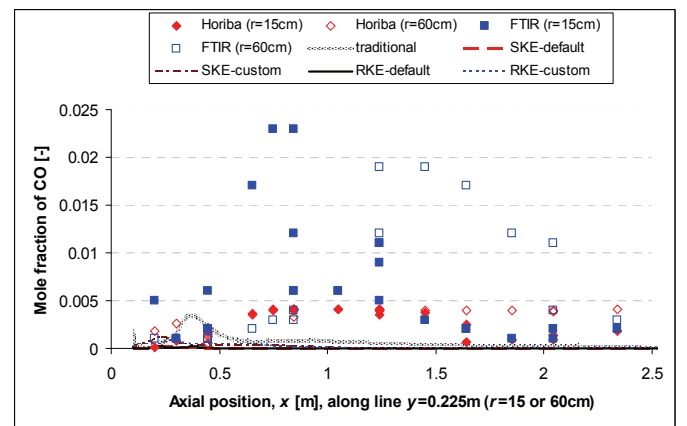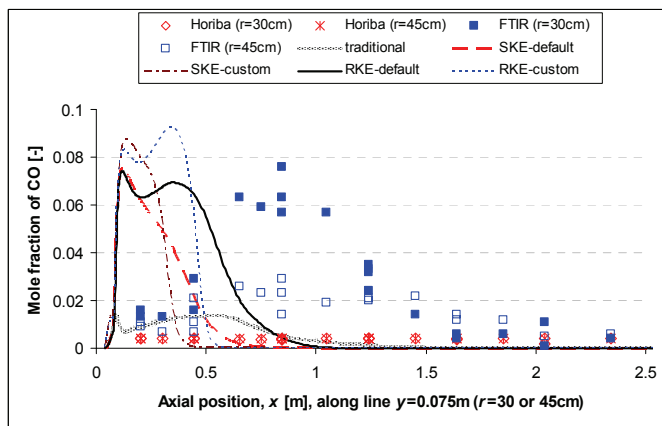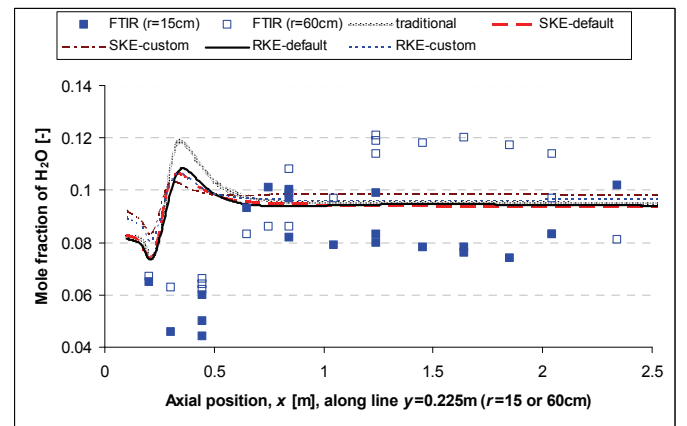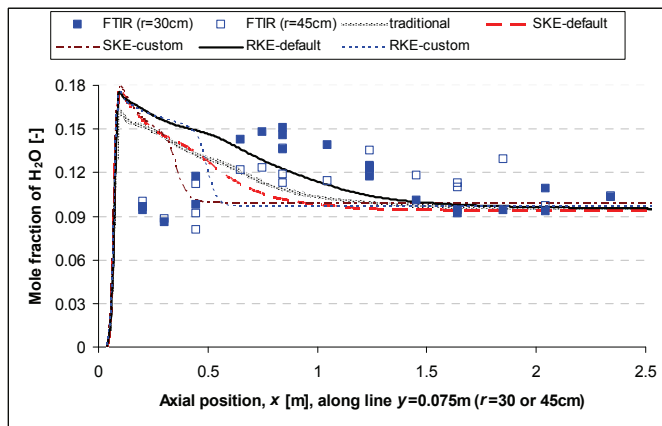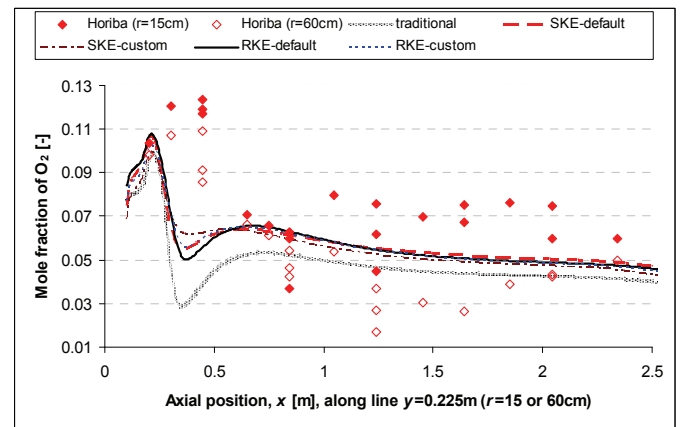
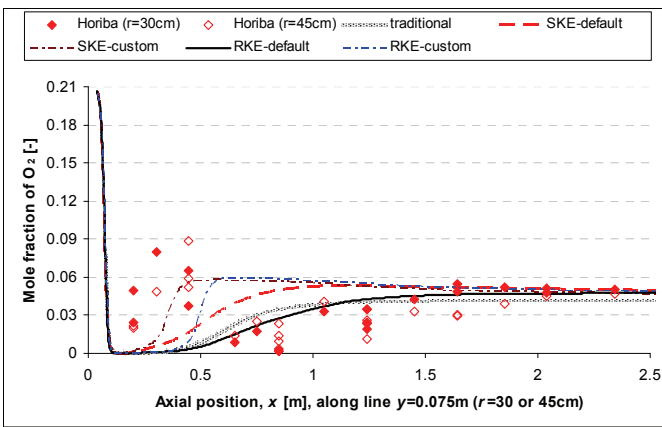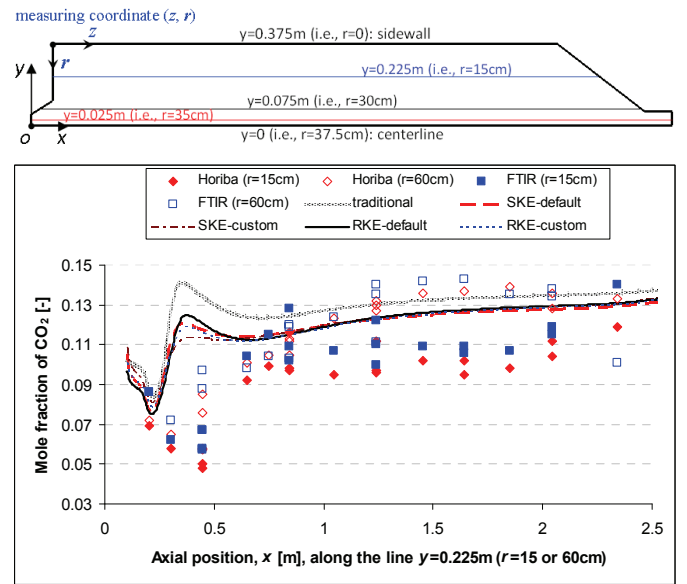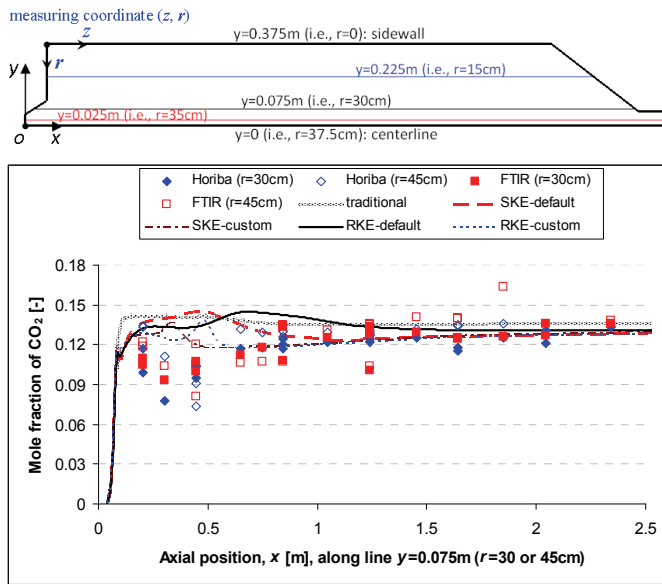Fig. 3 CFD *vs.* measurements on line *y=0.075m*

Fig. 4 CFD *vs.* measurements on line *y=0.225m*

The results of the custom particle conversion model show the temperature gradient inside the straw particles is small: only a few degrees in difference between the particle surface and the particle center. The reported straw char conversion rates in the reactor are also close to each other when different DPM laws are used for straw particle conversion. For instance, straw char conversion rates are 67% and 72% for the cases, "RKE-default" and "RKE-custom", respectively. As a result, the custom DPM laws may be expected not to have a big influence on the predicted gas species in the reactor. The relatively big difference, exhibited in Fig. 3, might be due to the too high DPM enthalpy source from the custom laws, in relative to the default laws.

- The four cases, which are based on Jones & Lindstedt's global reaction mechanism with EDC model used for turbulence-chemistry interaction, make significant difference with the "traditional" case which is based on simplified two-step mechanism with EDM. Jones & Lindstedt's four-step reaction mechanism was derived using analysis of flame structures and the final kinetic parameters for the resulting rate equations were determined by comparison with experimental data for premixed methane and propane flames, along with diffusion flame data for a methane-air flame. Their global reaction mechanisms have been found to have good agreement for a range of parameters such as flame speed, flame thickness, and species profiles [5]. Jones & Lindstedt's schemes are believed to perform much better than the over-simplified two-step global mechanism to describe high temperature oxidation of gaseous alkane hydrocarbons up to butane. EDM has been widely used in combustion simulation, for example [8], which presents also a CFD modeling of co-firing pulverized coal and biomass. EDM is used only in the "traditional" case in our study, for comparison. One of the drawbacks of EDM is the lack of generality of the model constants, A and B, which are very case-dependent. Moreover, EDM will most likely to produce incorrect solutions when multi-step reaction mechanisms are used [4]. Multi-step reaction mechanisms are based on chemistry kinetics, which differ for each reaction; whilst in EDM every reaction has the same, turbulent rate and therefore the same reaction rate. As a result, Jones & Lindstedt's reaction mechanism (i.e., mechanism-2) with EDC model is expected to better predict the species distribution than the simplified 2-step mechanism (i.e., mechanism-1) with EDM. Figures 3 and 4 do show this trend, from the comparison between the two cases, "traditional" vs. "RKE-default".

- There are still some discrepancies between the measured data and the CFD results, as shown in Fig. 3 and Fig. 4, which can be attributed to both the experimental and modeling sides. (1) From the geometries of the burner and reactor and the operational conditions, one would expect an axisymmetric combustion flow in the reactor, based on which axisymmetric swirl flow is used in all the CFD modeling. However, the measured mapping of the species indicates that the reacting flow in the reactor is not axisymmetric, which can also be seen in Fig. 3 and 4. (2) The measurements were done on different days. Though efforts were made to maintain the same operation conditions throughout the measuring period,

differences in operations were inevitable, which would lead to inconsistent measured results. (3) For the CFD modeling, the uncertainties with the fuels may be one of the major sources for the discrepancies. The two fuels are not really known well enough to carry out a reliable CFD modeling of such a co-firing flame, although the proximate analysis, the ultimate analysis and the particle sizes of both the fuels are given. The knowledge of the kinetic parameters (e.g., appropriate devolatilization and char oxidation sub-models) and the physical properties (e.g., particle density and specific heat) also plays a vital role in CFD modeling of solid fuel combustion and demands additional fuel characterization experiments. Unfortunately, most of the existing CFD modeling efforts for solid fuel combustion may have been done without such knowledge. In this study, we may argue that the CFD modeling could be based on the current best available knowledge of the kinetic parameters and the physical properties of the straw and coal fired in this reactor. The sensitivity study of those parameters, which is not presented in this paper, does show that they have very significant influence on the CFD results.

- As a conclusion of this section, "RKE-default" has been recommended as the baseline case at this stage, partly from expectation and partly from the comparison with the experimental data. This baseline case can be used for further investigation of the burner and also for the NO_x prediction. The detailed CFD results of "RKE-default" are shown in Fig. 5, along with those of the "traditional" case (shown in Fig. 6), which are used for comparison. Compared to the "traditional" case, the main reaction and flame predicted by "RKE-default" tend to be confined to a long and narrow core zone around the centerline of the reactor.

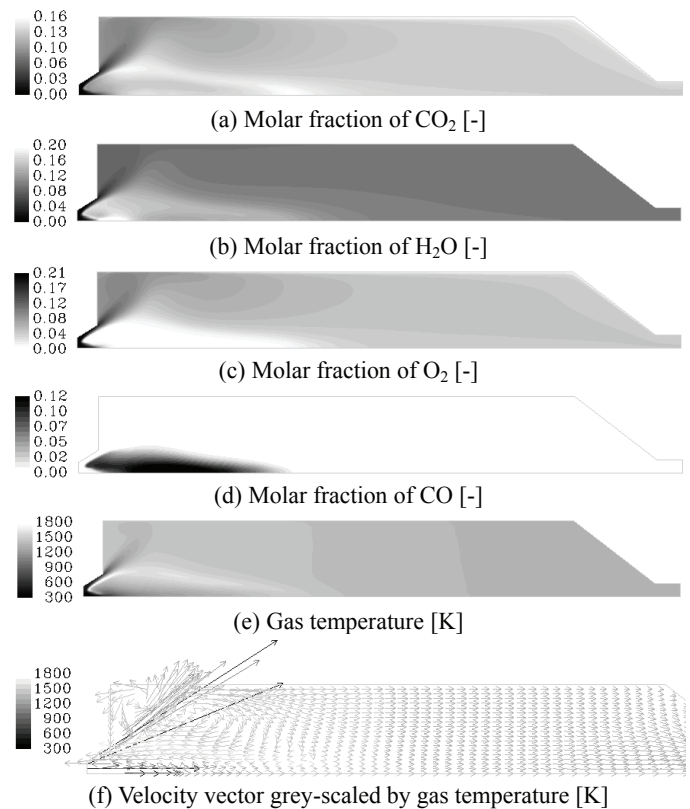(a) Molar fraction of CO_2 [-]

(b) Molar fraction of H_2O [-]

(c) Molar fraction of O_2 [-]

(d) Molar fraction of CO [-]

(e) Gas temperature [K]

(f) Velocity vector grey-scaled by gas temperature [K]

Fig. 5 CFD results of case "RKE-default"

(a) Molar fraction of CO_2 [-]

(b) Molar fraction of H_2O [-]

(c) Molar fraction of O_2 [-]

(d) Molar fraction of CO [-]

(e) Gas temperature [K]

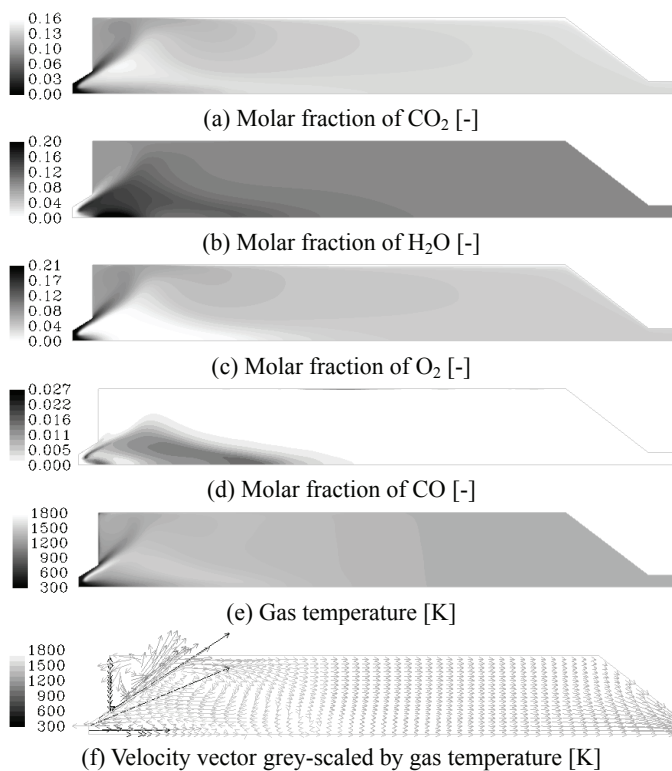(f) Velocity vector grey-scaled by gas temperature [K]

Fig. 6 CFD results of case "traditional"

6. CONCLUSIONS

A modeling approach for co-firing pulverized coal and biomass in swirling-stabilized burners is presented and demonstrated in this paper, in which realizable k-ε model is used for turbulence and Jones & Lindstedt's global reaction schemes with EDC model are used for homogeneous combustion of fuel-volatiles. The CFD results are calibrated first and then validated with measured gas species mapping. The following conclusions can be drawn from this study.

- Realizable k-ε model performs better than standard k-ε model in predicting swirling combustion flows, which is not surprising. However, the main difference is confined to the core zone. In the zone far away from the core zone, the difference is negligible.
- Although the simplified 2-step global mechanism with EDM has been very widely used in CFD modeling of industrial coal and/or biomass combustion processes, Jones & Lindstedt's global reaction schemes with EDC is expected to be a better option. Though Jones & Lindstedt's schemes can not be as generally applicable as detailed elementary mechanism, they do show excellent agreement with measured major species profiles for a wide range of premixed and non-premixed flames. As a result, Jones & Lindstedt's global schemes are expected to produce better combustion predictions than the over-simplified 2-step global mechanism. EDC model is general concept based on a detailed description of the dissipation of turbulent eddies, and allows for multi-step reaction mechanism. This study does demonstrate that Jones & Lindstedt's global reaction schemes with EDC model is a better option in predicting coal/biomass co-combustion flames.
- Knowledge about the solid fuels plays a vital role in CFD modeling of solid-fuel flames. However, such knowledge is very often incomplete. Besides the proximate analysis and ultimate analysis, additional fuel characterization experiments are absolutely needed to provide the knowledge of the kinetic parameters, as well as the physical properties of the solid fuels fired, in order to carry out a reliable CFD modeling. The sensitivity analysis done in this study does show that the kinetic parameters and the physical properties of the solid fuels have a great influence on the predicted species and temperature profiles. As demonstrated in our earlier work [3], the shape and size of biomass particles dramatically influence their trajectory and thus their conversion in a combustor. In this study, one could conclude that the intra-particle heat and mass transfer may be a secondary issue at most in the conversion of the biomass particles. For the straw particles fired in this reactor, the temperature differences inside the particles are quite small and the custom DPM laws do not really predict a significantly improved char conversion rate in this reactor, in comparison with the default DPM laws (72% in the former vs. 67% in the latter).
- More experiments are called for the study of pulverized coal and biomass co-combustion and its modeling, in order to provide more complete knowledge about the solid fuels themselves, to collect data for single biomass particle conversion, to produce consistent, quantitative maps of not only gas species but also gas temperature for the purpose of CFD validation.

8. REFERENCES

1. Yin, C., Rosendahl, L, Kær, S.K., Grate-Firing of Biomass for Heat and Power Production, Progress in Energy and Combustion Science, 34 (2008), pp.725-754.
2. Damstedt, B, Pedersen, J.M., Hansen, D., Knighton, T., Jones, J., Christensen, C., Baxter, L. Tree, D. Biomass cofiring impacts on flame structure and emissions. Proceedings of the Combustion Institute, 31 (2007), pp.2813-2820.
3. Yin, C., Rosendahl, L, Kær, S.K. and Condra, T., Use of Numerical Modeling in Design for Co-Firing Biomass in Wall-Fired Burners, Chemical Engineering Science, 59 (2004), pp.3281-3292.
4. FLUENT Inc., FLUENT 6.3.26 User's Guide, 2006.
5. Jones, W.P. and Lindstedt, R.P., Global Reaction Schemes for Hydrocarbon Combustion, Combustion and Flames, 73 (1988), pp.233-249.
6. Gera, D., Mathur, M.P., Freeman, M.C. and Robinson, A., Effect of Large Aspect Ratio of Biomass Particles on Carbon Burnout in a Utility Boiler, Energy & Fuels, 16 (2002), pp.1523-1532.
7. Di Blasi, C., Heat, Momentum and Mass Transport Through a Shrinking Biomass Particle Exposed to Thermal Radiation, Chemical Engineering Science, 51 (1996), pp.1121-1132.
8. Backreedy, R.I., Fletcher, L.M., Jones, J.M., Ma, L., Pourkashanian, M. and Williams, A., Co-Firing Pulverized Coal and Biomass: A Modeling Approach, Proceedings of the Combustion Institute, 30 (2005), pp.2955-2964.